

## Supplementary Information

# Chemical Analysis of Surface-Level Ozone Exceedances during the 2015 Pan American Games

**Craig A. Stroud** <sup>1,\*</sup>, **Shuzhan Ren** <sup>1</sup>, **Junhua Zhang** <sup>1</sup>, **Michael D. Moran** <sup>1</sup>, **Ayodeji Akingunola** <sup>1</sup>, **Paul A. Makar** <sup>1</sup>, **Rodrigo Munoz-Alpizar** <sup>2</sup>, **Sylvie Leroyer** <sup>3</sup>, **Stéphane Bélair** <sup>3</sup>, **David Sills** <sup>4</sup> and **Jeffrey R. Brook** <sup>5</sup>

<sup>1</sup> Air Quality Research Division, Environment and Climate Change Canada, Toronto, Ontario M3H 5T4, Canada; shuzhan.ren@canada.ca (S.R.); junhua.zhang@canada.ca (J.Z.); Mike.Moran@canada.ca (M.M.); Ayodeji.Akingunola@canada.ca (A.A.); paul.makar@canada.ca (P.M.)

<sup>2</sup> Meteorological Service of Canada, Environment and Climate Change Canada, Dorval, Quebec H9P 1J3, Canada; rodrigo.munoz-alpizar@canada.ca

<sup>3</sup> Meteorological Research Division, Environment and Climate Change Canada, Dorval, Quebec H9P 1J3, Canada; sylvie.leroyer@canada.ca (S.L.); stephane.belair@canada.ca (S.B.)

<sup>4</sup> Department of Civil and Environmental Engineering, University of Western Ontario, London, Ontario N6A 3K7, Canada; david.sills@umo.ca

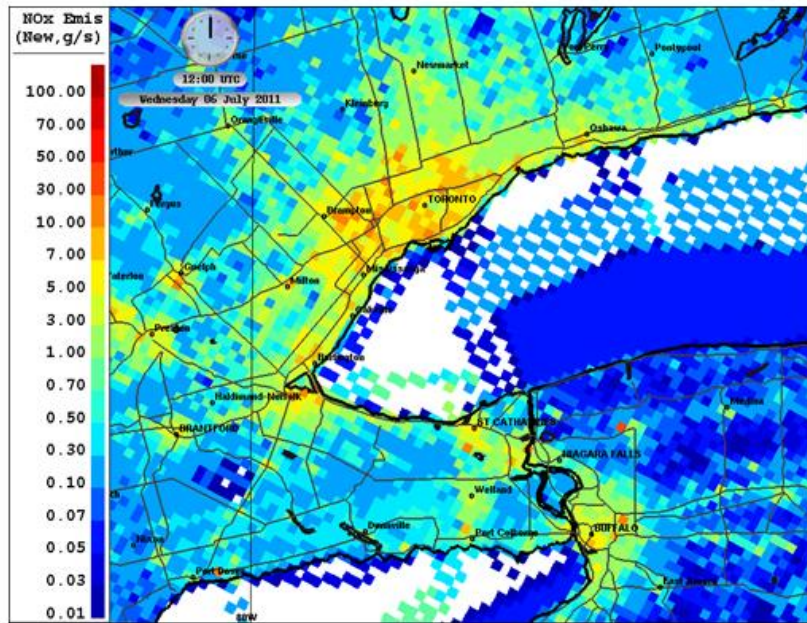
<sup>5</sup> Dalla Lana School of Public Health, University of Toronto, Ontario M5T 3M7, Canada; jeff.brook@utoronto.ca

\* Correspondence: craig.stroud@canada.ca; Tel.: +1-416-739-4849

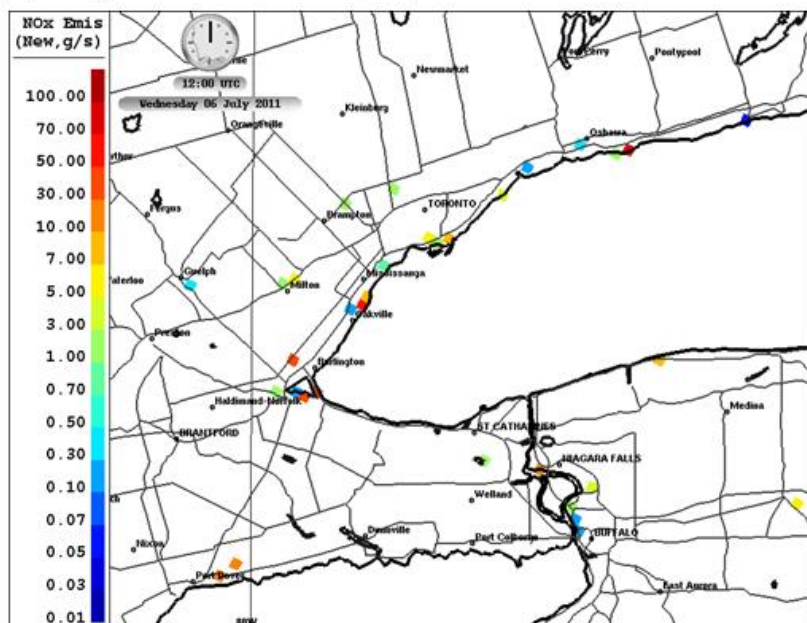
## Pollutant Emission Inventories and Emissions Processing for GEM-MACH-TEB

Figure S1 illustrates the spatial distribution of NO<sub>x</sub> emissions for a selected month, day, and hour for the GTHA and northwestern New York state. The highest NO<sub>x</sub> emission rates are found over the densely populated communities in Toronto and along major highways in the GTHA. The area southeast of Brampton has a high proportion of transportation-related NO<sub>x</sub> emissions due to the presence of Pearson International Airport, major railyards, and the intersections of several major highways. The area northwest of Hamilton has a concentration of point sources from the steel-production industry. There are also point sources from electric generation stations near Oakville and Oshawa along the lakeshore.

(a) NO<sub>x</sub> emission for area sources



(b) NO<sub>x</sub> emission for major point sources



**Figure S1.** NO<sub>x</sub> emission maps (g/s/grid cell) on the central portion of the 2.5-km grid for Month = July, Day = Wednesday, Time = 12:00 UTC. Panel (a) includes all area sources. Panel (b) illustrates all

the major point sources, color-coded as a function of NO<sub>x</sub> emission rate (g/s). The black lines are major roads.

### **Emission Trends for O<sub>3</sub> Precursors over the Last Decade**

NO<sub>x</sub> emissions, over the entire province of Ontario, decreased by 38% between 2006 and 2015 [1]. This is mostly from decreases in NO<sub>x</sub> emissions from on-road vehicles and coal-burning electricity utilities. In the neighboring U.S. state of Ohio, emissions of NO<sub>x</sub> decreased by 60% between 2006 and 2015 [2]. Similar to NO<sub>x</sub>, emissions of carbon monoxide for Ontario decreased by 32% between 2006 and 2015 [1]. In the U.S., emissions of total anthropogenic VOC in Ohio decreased by 21% between 2006 and 2015 [2]. In Canada, the trend for annual mean toluene concentration for NAPS sites across Ontario decreased 54% (3.0 µg/m<sup>3</sup> to 1.4 µg/m<sup>3</sup>) from 2005 to 2014 [3]. The U.S. NO<sub>x</sub> emission trend data for all source sectors is now available up to year 2017 [4]. For the state of Ohio, the total NO<sub>x</sub> emission for years 2015 and 2017 were 348 kt and 317 kt, respectively (-8.9% change). Thus, our use of projected 2017 U.S. emissions should not affect our model simulation for summer 2015 by a significant extent.

### **GEM-MACH-TEB Model Evaluation Using All the Available Hourly Data for the 12 GTHA Sites**

The performance metrics used to evaluate model performance in this study are similar to the metrics used in other studies (e.g., [5-8]). Table S1 presents the 2.5-km GEM-MACH-TEB model statistical comparisons to the hourly NAPS observations aggregated for the 12 urban and suburban sites in the GTHA. The normalized mean bias (NMB), correlation coefficient (R) and root mean square error (RMSE) scores are shown, for O<sub>3</sub>, NO<sub>2</sub>, NO<sub>x</sub>, and O<sub>x</sub>. NO<sub>x</sub> and O<sub>x</sub> are longer-lived quantities, largely independent of the rapid photo-stationary state cycling between NO, NO<sub>2</sub> and O<sub>3</sub>. O<sub>x</sub> is also independent of short-term, localized emissions of NO. Similarly, NO<sub>x</sub> is independent of short-term changes in radiation intensity. Since NO<sub>x</sub> and O<sub>x</sub> are more spatially homogeneous with slower time variations, they are appropriate quantities to compare to gridded chemical transport model output. In looking at the NO<sub>x</sub> statistics for the GTHA sites, the average model NMB and correlation R, are -0.7% and 0.65, respectively. The modeled mean NO<sub>x</sub> using the hourly data from the GTHA sites over the month of July is 13 ppbv. Collectively, the model predicts a small negative O<sub>x</sub> bias (NMB - 5.3%) and a strong correlation (R = 0.82) for the GTHA sites. In looking at the O<sub>3</sub> and NO<sub>2</sub> statistics, the model over-predicts NO<sub>2</sub> (NMB +13.1%) and under-predicts O<sub>3</sub> (NMB -10.5%). The O<sub>3</sub> and NO<sub>2</sub> correlations are also both strong, 0.81 and 0.74, respectively. The NO<sub>x</sub> correlation coefficient is the lowest of all the species due to it having the steepest spatial gradient of all the species, which requires accurate model forecasts for wind direction and depth of vertical mixing.

Table S1 also compares the scores for the 2.5-km nested GEM-MACH-TEB to the 10-km GEM-MACH piloting model for the 12 GTHA sites. Both models were based on GEM v4.8.3 and used the same emission inventories. The outer model is analogous to the operational version of GEM-MACH used by the Meteorological Service of Canada for AQHI forecasting. The higher resolution model performs better for bias and error statistics for O<sub>3</sub> and NO<sub>2</sub>. Only for the grouped species (O<sub>x</sub>) does the high resolution perform slightly worse for bias, although both biases are good. However, the correlation coefficient is slightly worse for the high resolution compared to the lower resolution version. This is not surprising giving the plume-like nature of urban air masses and the challenge in predicting the wind direction needed to precisely model plume dispersion. The lower resolution model is more forgiving in terms of imprecision in the wind direction and still having an impact on a receptor site. A detailed discussion of such effects and comparisons between lower and higher resolution simulations may be found in [9].

Another metric impacted by model spatial resolution is the standard deviation around the mean predicted value, particularly for primary emitted species. The standard deviation is a measure of the variability, which is impacted by urban plume width and the model's ability to capture the peak value in the center of the plume. The measured NO<sub>x</sub> mean standard deviation is 5.9 ppbv. Similarly,

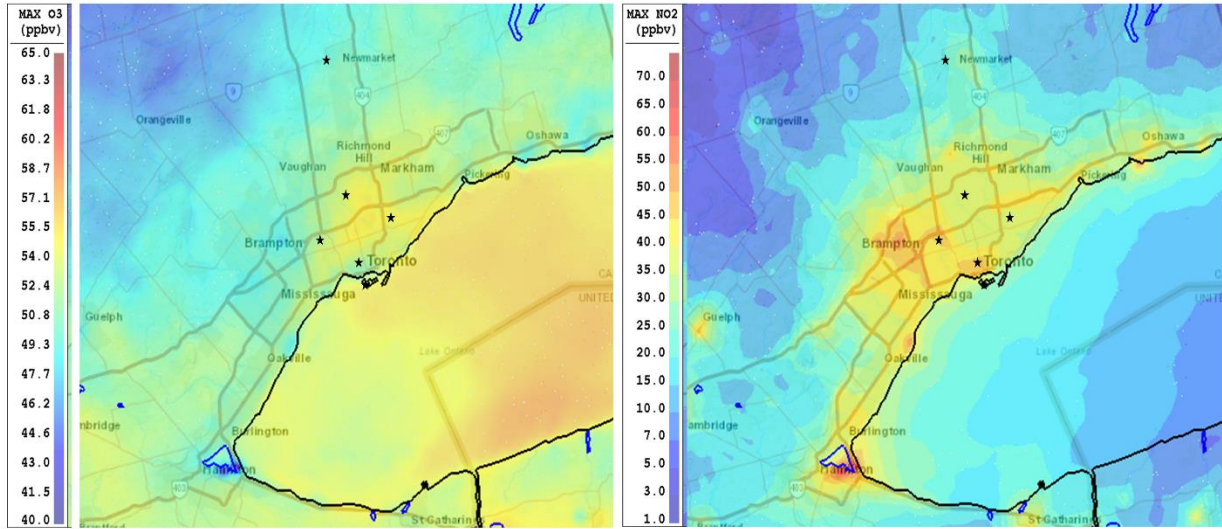
the high spatial resolution model has a smaller standard deviation, 7.2 ppbv, compared to 8.3 ppbv for the 10-km piloting model.

**Table S1.** Comparison of 10-km GEM-MACH with 2.5-km GEM-MACH-TEB model scores for the 12 GTHA sites. Values in red font denote better scores between the two model configurations.

Pollutant	Metric	Locations Observed Mean and Standard Deviation (ppbv)	Model Mean and Standard Deviation (ppbv)	NMB (%)	Correlation Coefficient, R	RMSE (ppbv)
2.5-km GEM- MACH-TEB	O <sub>3</sub> 1-h data,	GTHA 31.6 ± 7.7	28.3 ± 9.3	-10.5	0.81	6.4
10-km Operational	Entire month		26.3 ± 8.9	-16.8	0.78	8.2
2.5-km GEM- MACH-TEB	NO <sub>2</sub> 1-h data,	GTHA 8.4 ± 3.5	9.5 ± 4.7	+13.1	0.74	3.7
10-km Operational	Entire month		11.3 ± 5.4	+46.4	0.77	5.7
2.5-km GEM- MACH-TEB	NO <sub>x</sub> 1-h data,	GTHA 13.1 ± 5.9	13.0 ± 7.2	-0.7	0.65	6.7
10-km Operational	Entire month		17.5 ± 8.3	+33.6	0.68	9.6
2.5-km GEM- MACH-TEB	O <sub>x</sub> 1-h data,	GTHA 39.9 ± 8.2	37.8 ± 10.0	-5.3	0.82	6.2
10-km Operational	Entire month		38.6 ± 10.9	-3.3	0.84	6.8

### Model Evaluation using O<sub>3</sub> Air Quality Metrics for Toronto Measurement Sites

The Ontario ambient air quality standard for O<sub>3</sub> is based on the daily 1-h max. of 80 ppbv. Figure S2a shows the map of the monthly mean of the daily 1-h O<sub>3</sub> maximum for July 2015. The highest O<sub>3</sub> mixing ratios are predicted over Uptown Toronto and North Toronto and over Lake Erie and Lake Ontario. Figure S2b shows the corresponding monthly mean map of the daily 1-h NO<sub>2</sub> maximum for July 2015. The highest NO<sub>2</sub> mixing ratios are local to the Hamilton steel production facilities, to the intersections of several major highways and near the Pearson International Airport in Brampton. Table S2 presents the model performance in predicting the daily 1-h O<sub>3</sub> max. for July 2015 for the four measurement sites in the GTHA that lie along a line away from Toronto Island to Downtown Toronto to North Toronto to the suburban town of Newmarket (see Figure 2). The O<sub>3</sub> NMB for the North Toronto and Downtown Toronto sites were similar, -6.8% and -5.6%, respectively. The Newmarket site had a small negative NMB of -0.8 %, and the Toronto Island site had an NMB value of +3.1%. The Toronto Island positive bias for a lake-impacted site compares better than other studies that have predicted much higher O<sub>3</sub> biases over the Great Lakes region [10,11]. The RMSE scores in Table S2 for all four sites are in the range 8.9 to 10.5 ppbv. Overall, the statistics for the predicted daily 1-h maxima can be considered good compared to prior studies in literature [5]. The mean measured daily 1-h O<sub>3</sub> maxima is highest for the North Toronto site (56 ppbv) and lowest for the Newmarket location (48 ppbv). The model is able to capture this spatial difference for these two sites, which are about 30 km apart.

(a) Mean Daily 1-h Max. O<sub>3</sub>(b) Mean Daily 1-h Max. NO<sub>2</sub>

**Figure S2.** Monthly mean maps for daily 1-h maximum for O<sub>3</sub> (panel a) and NO<sub>2</sub> (panel b) for July 2015. The stars are the locations of measurement stations discussed in text (refer to Figure 2 for names). The thick line over Lake Ontario is the U.S./Canadian border.

**Table S2.** Model evaluation scores for daily 1-h ozone maximum for 4 selected sites in the GTHA for July 2015.

Pollutant	Metric	Observed Mean and Standard Deviation (ppbv)	Model Mean and Standard Deviation (ppbv)	NMB (%)	Correlation Coefficient R	RMSE (ppbv)
O <sub>3</sub>	Daily 1-h-max.	North Toronto 56 ± 15	52 ± 17	-6.8	0.85	9.5
		Downtown 52 ± 14	49 ± 15	-5.6	0.76	10.5
		Newmarket 48 ± 13	47 ± 16	-0.79	0.82	8.9
		Toronto Island 50 ± 13	52 ± 15	3.1	0.81	9.0

The Canadian Ambient Air Quality Standard (CAAQS) for O<sub>3</sub> is the 3-year running average of the 4th highest daily maxima 8-h average (DM8A). The current standard is set at 63 ppbv. Figure S3 illustrates the modelled DM8A values plotted against the observed values for the North Toronto site. It can be seen that four days surpass the metric of 63 ppbv. Overall, the correlation coefficient (0.86), slope (0.94) and intercept (-1.2 ppbv) are modeled well. Figure S4 is the corresponding plot for the Downtown Toronto location. The correlation coefficient is a little lower (0.81) but, overall, the model performance in predicting the DM8A O<sub>3</sub> mixing ratio is very good and comparable to other recently published AQ forecasting systems [12]. Table S3 shows the DM8A statistics for other sites in Toronto. The NMB for the Newmarket suburban site is small, -2.5 %, while Toronto Island has a NMB of -0.95 %. The correlation coefficients in Table S3 are all above 0.8. The highest observed monthly mean DM8A value occurs at the North Toronto site and the lowest at Newmarket. The modeled mean DM8A values are similar for North Toronto and Toronto Island and higher than Downtown Toronto and Newmarket.

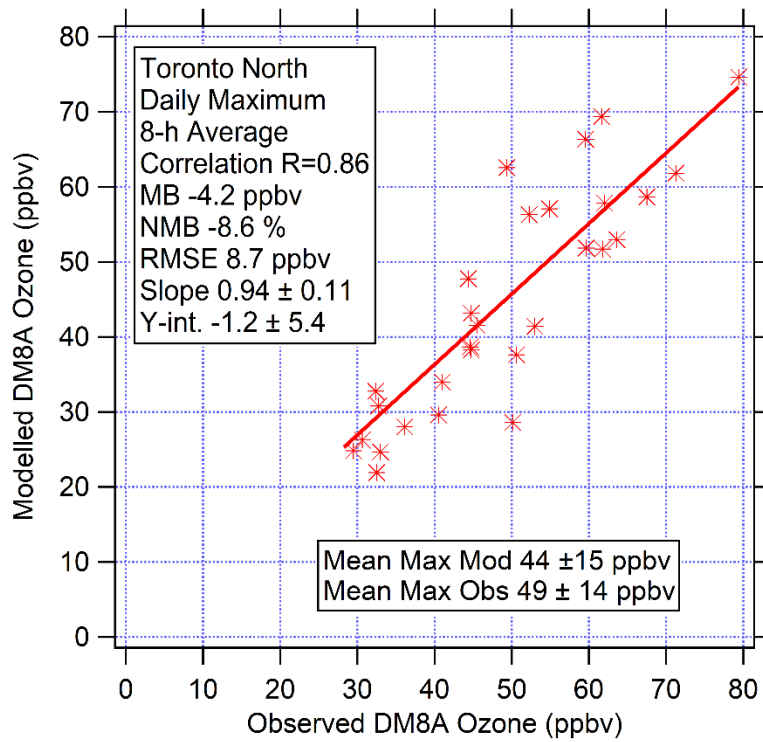


**Figure S3.** Ozone model/measurement correlation plot for Toronto North site. DM8A is the Daily Maximum 8-h Average.

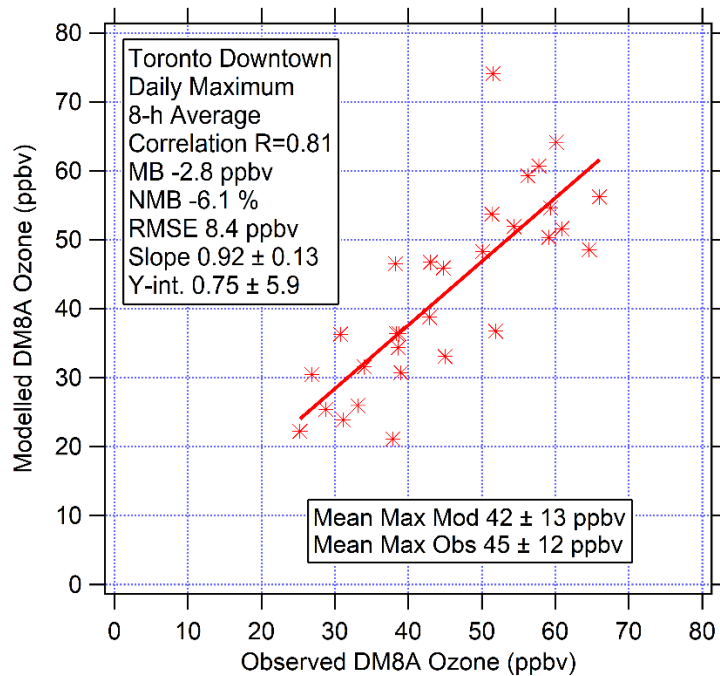


**Figure S4.** Ozone model/measurement correlation plot for Toronto Downtown site. DM8A is the Daily Maximum 8-h Average.

A recent study evaluated the ozone performance of the CMAQ model (4-km grid spacing) for the Lake Michigan region and performed a series of sensitivity tests with refined biogenic VOC emissions, on-road mobile  $\text{NO}_x$  emissions, updated gas-phase chemistry mechanism, and higher  $\text{O}_3$  dry deposition to lake surfaces [12]. Our DM8A results for North Toronto for R (0.86) and RMSE (8.7 ppbv) are slightly better than the CMAQ model results for their shoreline site category (R = 0.6 and

RMSE = 13.5 ppbv). Our O<sub>3</sub> NMB results (-10.5%) in Table S2 are comparable in magnitude to the recently published CMAQ bias (NMB +8.8%). It should be noted, however, that the geographic location and the month used for the evaluation is different.

The DM8A O<sub>3</sub> values occur during daytime hours, usually between 11:00 a.m. and 07:00 p.m. local time. The NO<sub>x</sub> predicted during these hours is thus important to consider and evaluate. The statistics for the daytime maximum 8-h average NO<sub>x</sub> concentration (11:00 a.m.–07:00 p.m. local time) for the Toronto sites are also presented in Table S3. The correlation coefficient and RMSE values are similar for the Downtown and North Toronto sites, falling in the range 0.59–0.68 and 3.7–4.0 ppbv, respectively. However, the North Toronto site has a negative NMB of -18.3 % whereas the Downtown Toronto site has only a small negative NMB of -0.92 %. The small bias for the downtown location is consistent with the CRUISER data for the downtown grid cell (Section 3.1). Of the 4 sites in Table S3, the suburban Newmarket site has the lowest measured and modelled daytime maximum 8-h average NO<sub>x</sub> mixing ratios, 3.6 and 3.2 ppbv, respectively. The NMB for Newmarket is -11.3 %. A negative model bias might be expected for a rural/suburban site, like Newmarket, given the hypothesized positive NO<sub>2</sub> measurement bias for instruments using non-specific NO<sub>2</sub> to NO converter techniques [13], as these can also convert some of the other odd nitrogen species (e.g., peroxyacetal nitrate species) to NO. Rural/suburban sites, compared to urban sites, have more oxidized odd nitrogen species relative to freshly emitted NO<sub>x</sub> species and, thus, rural/suburban sites can have NO<sub>x</sub> measurements biased high, which can lead to model under-prediction. The correlation R of 0.73 at Newmarket is the best of the four sites. Newmarket experiences the widest dynamic range for NO<sub>x</sub>, as the site samples very clean air from northerly directions and polluted air from southerly directions.

Table S3. Model evaluation for daily maximum 8-h average O<sub>3</sub> and NO<sub>x</sub> mixing ratios for four selected sites in GTHA for July 2015. Obs. is Observed

Pollutant	Metric	Location Observed Mean and Standard Deviation	Mean and Standard Deviation (ppbv)	NMB (%)	Correlation Coefficient R	RMSE (ppbv)
O <sub>3</sub>	Daily max 8-h-average	North Toronto 49 ± 14	44 ± 15	-8.6	0.86	8.7
		Downtown 45 ± 12	42 ± 13	-6.1	0.81	8.4
		Newmarket 43 ± 11	42 ± 14	-2.5	0.86	7.4
		Toronto Island 45 ± 12	45 ± 14	-0.95	0.83	7.5
NO <sub>x</sub>	Daytime 8-h- average from 11:00 a.m.– 07:00 p.m.	North Toronto 8.4 ± 4.7	6.9 ± 3.1	-18.3	0.68	3.7
		Downtown 11.6 ± 4.9	12 ± 4.2	-0.92	0.59	4.0
		Newmarket 3.6 ± 2.2	3.2 ± 2.6	-11.3	0.73	1.8
		Toronto Island 5.0 ± 3.1	5.2 ± 3.3	2.7	0.63	2.7

### U.S. EPA Model Performance Guidelines for Surface Ozone

A model evaluation guidance document published by the U.S. EPA [14] is often considered by the air quality modeling community in performance evaluations. The performance criteria guidelines for O<sub>3</sub> are a mean fractional error of less than 35% and a mean fractional bias of ±15%. The model O<sub>3</sub> predictions for all sites in Ontario, using the entire 1-h data sets for July 2015, are just slightly higher than the benchmark for both mean fractional error (36%) and mean fractional bias (-16%). However, if nighttime data points with O<sub>3</sub> observations less than 20 ppbv are removed from the analysis, then

the model meets the performance criteria (MFE = 27%, MFB = -15%). The implementation of an O<sub>3</sub> cutoff value for background O<sub>3</sub> is recommended by the U.S. EPA guidance document to assess daytime O<sub>3</sub> predictions, while at the same time removing nighttime O<sub>3</sub> predictions that are often biased low due to the model's inability to resolve fine-scale mixing processes near the surface under stable conditions. Our model results are similar to other recent studies in the literature [15], which also used a lower limit cutoff and compared to the U.S. EPA guidelines.

The Supplemental Information also includes an evaluation of O<sub>x</sub> predictions grouped according to three different wind conditions (southwesterly, northerly, and light wind speeds from any direction) and two temporal periods (mid-morning and mid-afternoon). The modelled wind data were stratified using these criteria and paired with the coincident measured wind data for the entire month of July. O<sub>x</sub> biases for the six conditions ranged from -7.3 ppbv (light wind group, afternoon group) to -1.0 ppbv (south wind group, afternoon group). The light wind condition had the highest observed afternoon O<sub>x</sub> and the model also predicted the highest O<sub>x</sub> for this condition. The southwesterly wind direction had the second highest observed afternoon O<sub>x</sub> and the model O<sub>x</sub> agreed quite well for this wind direction (average bias -1.0 ppbv). The northerly wind direction had the lowest afternoon O<sub>x</sub> average and the model also predicted the lowest O<sub>x</sub> for this condition.

### **Model Performance for Different Meteorological Conditions**

It is interesting to compare the modeled and observed O<sub>x</sub> mixing ratios grouped for different meteorological conditions and calculate the O<sub>x</sub> biases [16]. The selection of data for different wind conditions helps to separate the O<sub>x</sub> data by its source regions. Here, the North Toronto site is selected because it receives less impact from pollutant emissions with a north wind direction than a south wind direction; thus, one direction represents polluted conditions and the other direction cleaner conditions. Figure S5 is the change in average modeled and observed O<sub>x</sub> mixing ratios for two time periods of the day (morning, 2 to 6 am and afternoon, 2 to 6 pm) and for 3 different wind conditions (northerly wind between 270° to 45° and greater than 8.0 knots (4.1 m/s), southerly wind between 135° to 270° and greater than 8.0 knots (4.1 m/s), and a light wind < 8 knots) at the North Toronto location for July 2015. The averages are for the entire July period. For each wind condition, there are the same number of model and measurement points used to calculate the average. For the northerly wind condition, the model predicts a similar change in average O<sub>x</sub> from early morning to afternoon; however, the model has a negative bias of 6–8 ppbv. This difference in background O<sub>x</sub> is quite large and should be examined more in future work.

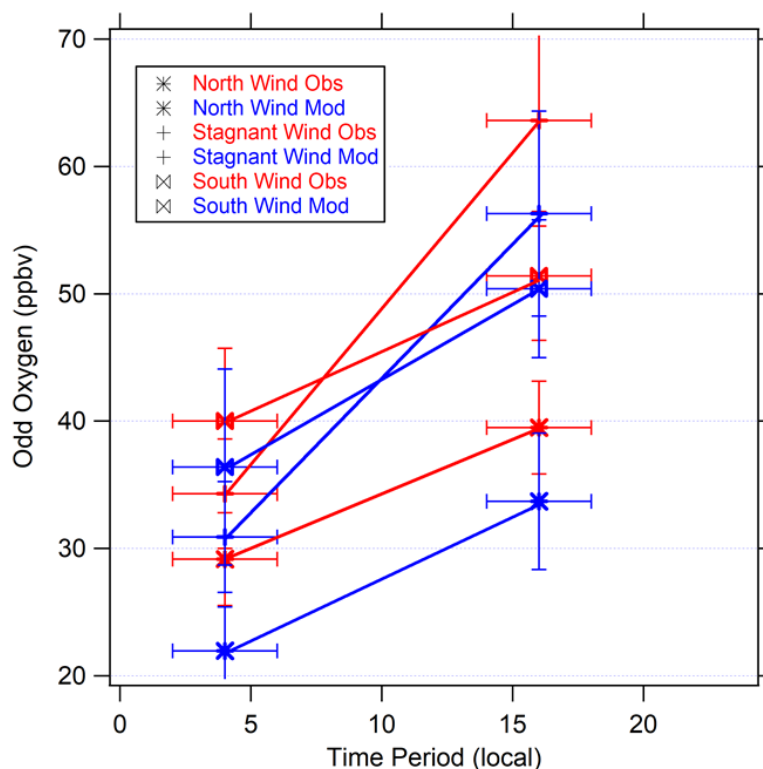


**Figure S5.** Odd Oxygen ( $O_x$ ) mixing ratio averaged for two time periods of day and for different wind conditions (north sector, south sector, stagnant). Model results for July 2015 are displayed in blue and observations in red. Early morning 02:00–06:00 a.m., Afternoon 02:00–06:00 p.m.

The afternoon average  $O_x$  is predicted quite well for the south wind direction.  $O_x$  from this wind direction is likely influenced more from long-range transport from high pollutant emission regions in southern Ontario and Ohio.

For a stagnant wind, local production is most important and the afternoon observed  $O_x$  is highest for this wind condition and the model under-predicts average  $O_x$  by 7 ppbv. The morning average  $O_x$  is under-predicted by 4 ppbv for the light wind condition. For the light wind days, the pollutants emitted from Toronto in the early morning are transported out over the lake. Later in the morning, the polluted air mass is transported back on-shore over Toronto, resulting in the further accumulation of primary pollutants from urban sources. The lake-breeze circulation can also last over several days, resulting in further concentration of emitted pollutants in the same air mass. In this way, after several light wind days, there can be large  $O_3$  increases from the accumulation of local emissions caught in the lake-breeze circulation. This pattern was also observed during the BAQS-Met field study [17]. The increase in  $O_3$  for the light wind condition between morning and afternoon is calculated to be 3 ppbv/h in Figure S5 and this increase is similar for both observations and model.

### Air Mass Back Trajectories calculated with the HYSPLIT Model

The U.S. National Oceanic and Atmospheric Administration (NOAA) provides the capability to calculate meteorological back trajectories using the HYSPLIT (Hybrid Single Particle Lagrangian Integrated Trajectory) model (<https://ready.arl.noaa.gov/hypub-bin/trajtype.pl>) with different selections for archived meteorological data. Figure S6 shows a back trajectory ending at 20:00 UTC on 28 July 2015 using the 12-km resolution North American Mesoscale Forecast System (NAM) meteorological data. The end-point is the North Toronto site using a final altitude of 100-magl. The backward trajectory was run for 48-h using the modeled vertical velocity option. The NAM-based trajectory originates over northern Lake Huron two days prior and travels southeast to a point over Lake Ontario before turning back NW towards Toronto. The trajectory actually crosses directly over

Toronto on its southward trajectory and then switches north in the lake-breeze front and retraces its path to North Toronto. The backward trajectory with the 3-km HRRR (High Resolution Rapid Refresh) meteorological data option in HYSPLIT is similar, but travels southeast to a point farther west over Lake Ontario and then turns in a more northerly direction towards Toronto.

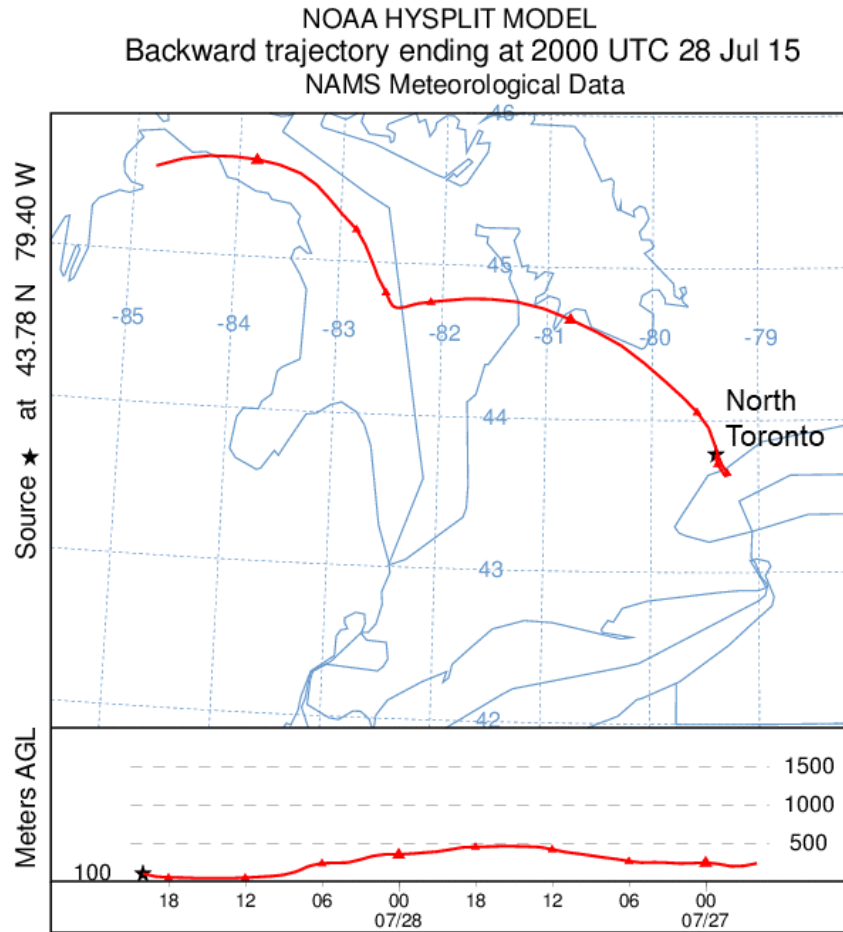


**Figure S6.** 48-h back-trajectory for air ending at the North Toronto site at 100-m AGL on the afternoon of 28 July 2015. Triangles mark 6-hourly positions. Data from the 12-km NAMS analysis is used.

NOAA HYSPLIT MODEL  
Backward trajectory ending at 2000 UTC 28 Jul 15  
HRRR Meteorological Data

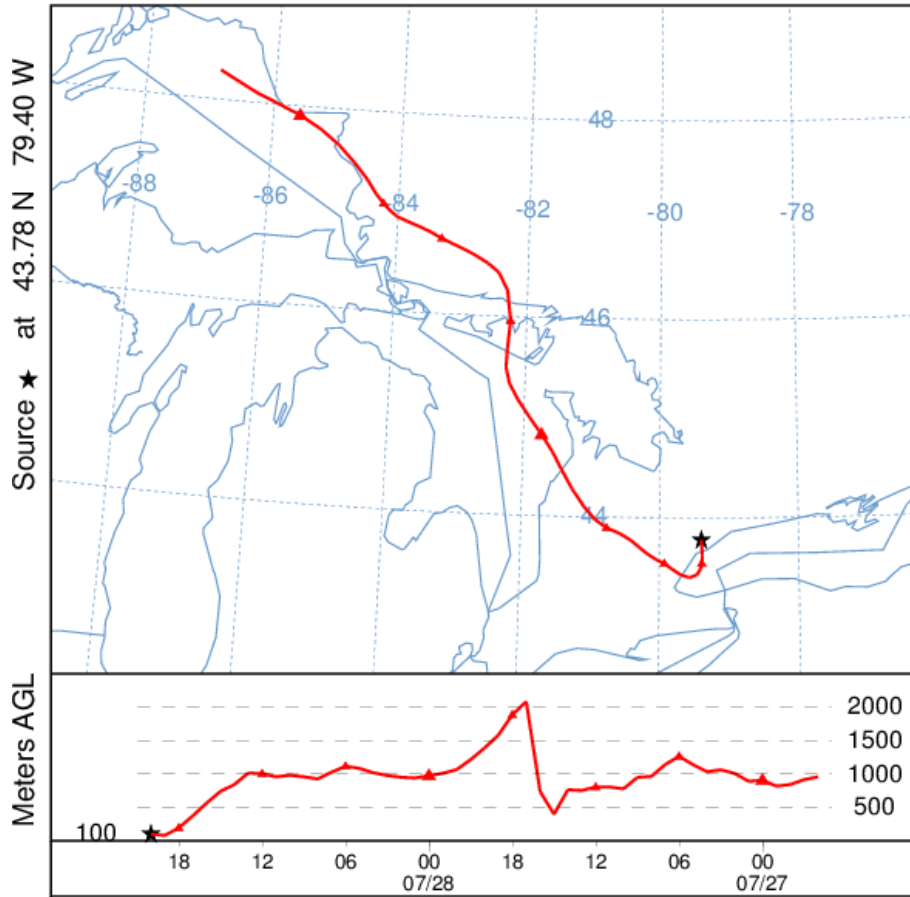


**Figure S7.** 48-h back-trajectory for air ending at the North Toronto site at 100-m AGL on the afternoon of 28 July 2015. Data from the 3-km HRRR analysis is used. Triangles mark 6-hourly positions.

NOAA HYSPLIT MODEL  
Backward trajectory ending at 2000 UTC 12 Jul 15  
NAMS Meteorological Data

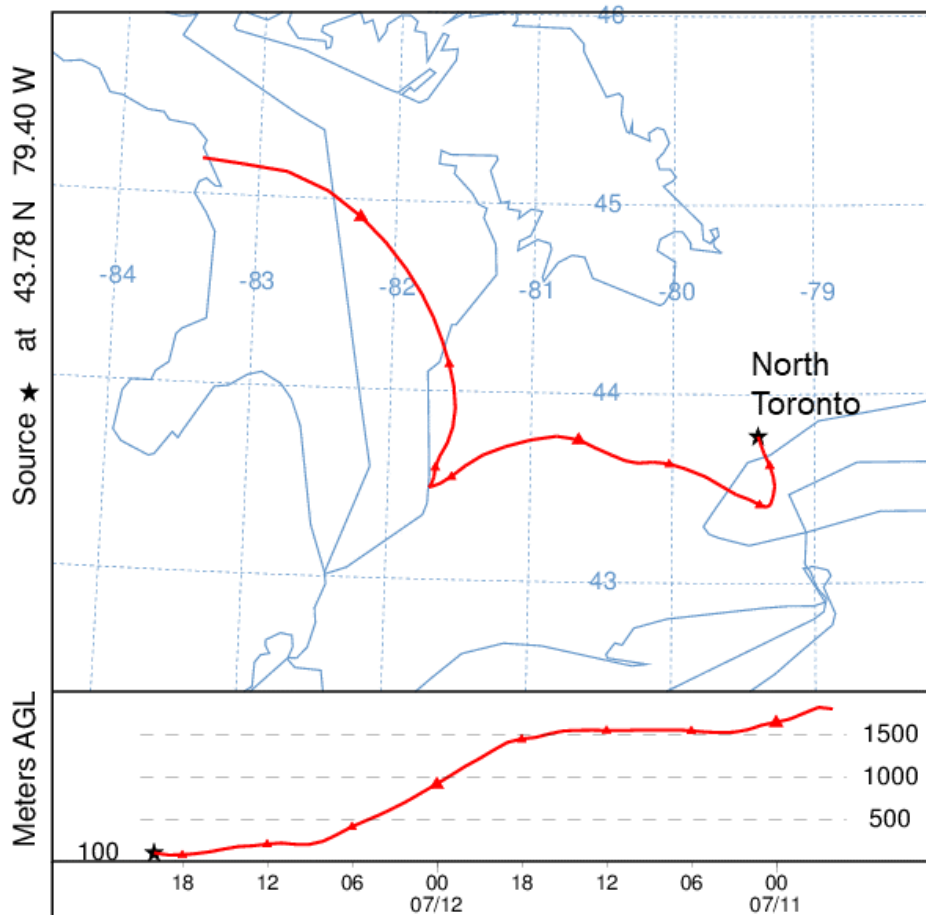


**Figure S8.** 48-h back-trajectory for air ending at the North Toronto site at 100-m on the afternoon of 12 July 2015. Data from the 12-km NAMS analysis is used.

NOAA HYSPLIT MODEL  
 Backward trajectory ending at 2000 UTC 12 Jul 15  
 HRRR Meteorological Data

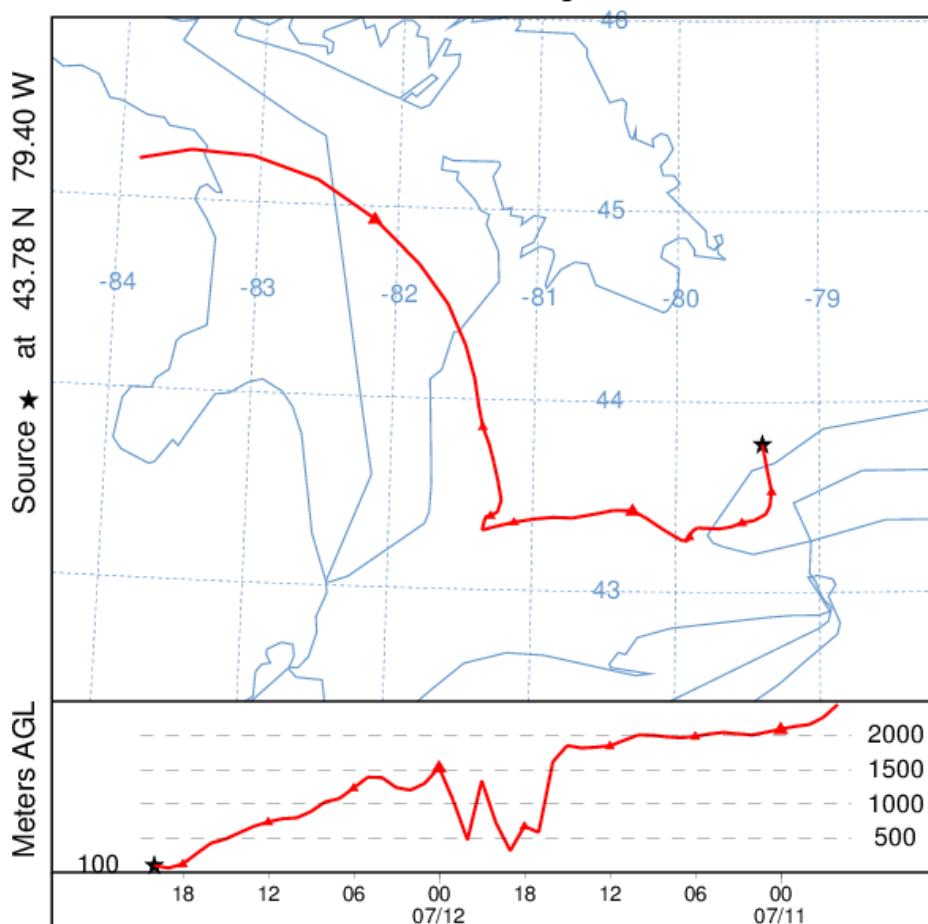


**Figure S9.** 48-h back-trajectory for air ending at the North Toronto site at 100-m on the afternoon of 12 July 2015. Data from the 3-km HRRR analysis is used.

**Meteorological and Chemical Conditions leading up to O<sub>3</sub> Exceedance on 28 July 2015**

The weather was calm at 12:00 UTC (08:00 a.m. local time) on 28 July with light surface winds from the northwest over Toronto (arrows in Figure S10). All the same-quantity panels (e.g., Figures S10a, S12a, S14a, and 13a) have the same color-scale so that differences at different times are evident. Winds at 2-km altitude were from the NNE over the region. An urban heat island is evident over Toronto with temperatures 2 °C warmer than the suburbs. The primary emitted pollutants, NO<sub>x</sub> and VOCs (represented by the model TOLU species “Toluene + Other Mono-substituted Aromatics”), were concentrated in a shallow surface layer with northwesterly winds associated with the nighttime land breeze transporting pollutants out over Lake Ontario (Figure S11). The mixing length over the lake was very low (Figure S10d). Mixing length is a measure of turbulent motion in an air parcel. Large concentration gradients are modelled in the lowest 300-m depth over Toronto Island. The predicted O<sub>3</sub> was very low over the entire GTHA in the lowest 300-m due to fast reaction of O<sub>3</sub> with freshly emitted NO (i.e., NO titration). The O<sub>3</sub> in the residual layer over Toronto and Lake Ontario was modeled in the 35–45 ppbv range. The O<sub>3</sub> above 2-km altitude in the NNE wind was the highest, at 40–50 ppbv, from longer-range transport.

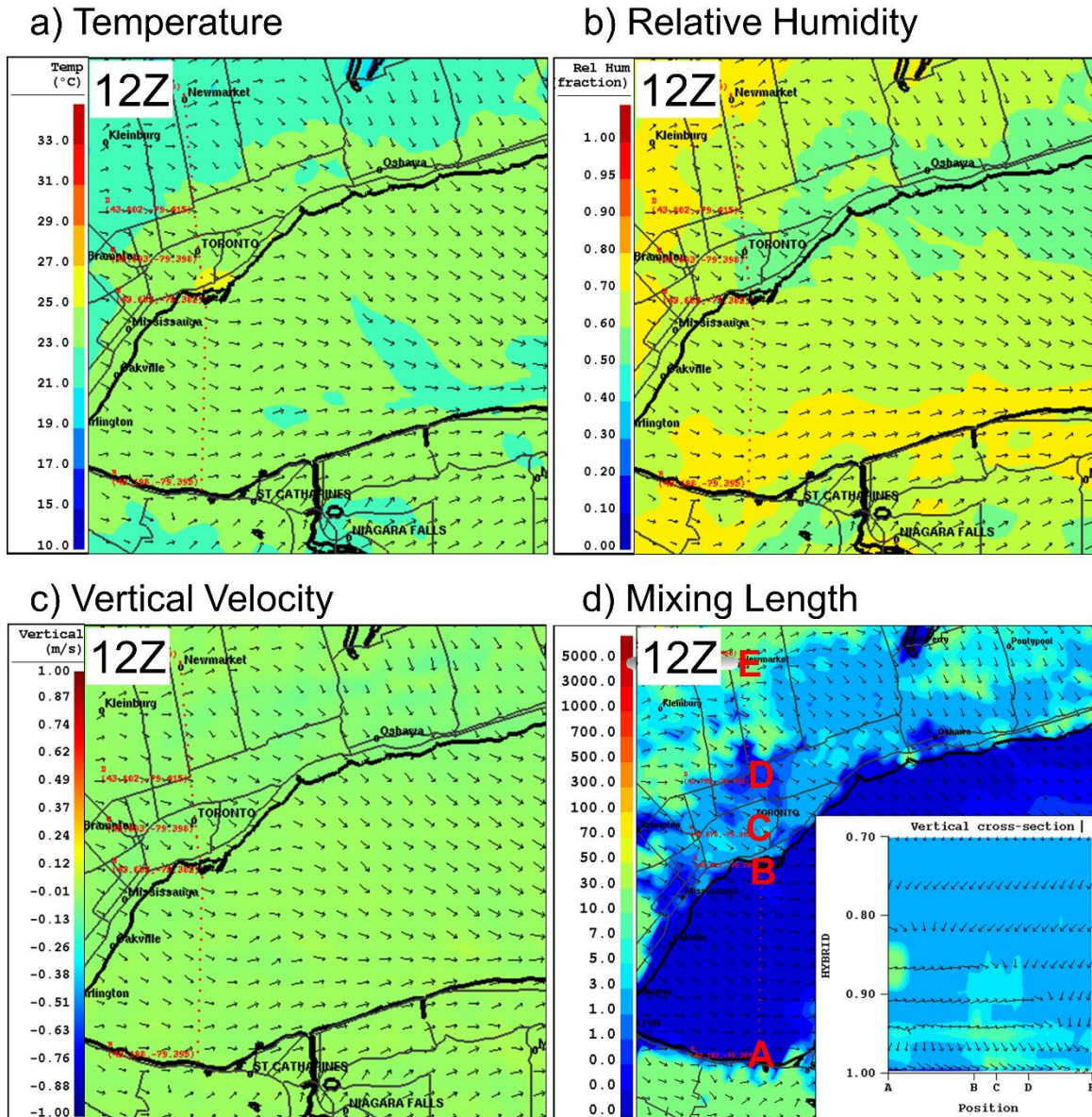


**Figure S10.** GEM-MACH-TEB predictions for meteorological variables at 12:00 UTC 28 July 2015. Panels are for (a) surface air temperature ( $^{\circ}\text{C}$ ), (b) surface relative humidity (as a fraction), (c) vertical wind velocity at 300-m (m/s), and (d) surface turbulent mixing length (meters). The inset vertical cross section in panel (d) extends from point A (south shore of Lake Ontario) to B (Toronto Island), C (Downtown Toronto), D (North Toronto) and E (Newmarket). The white line shown in panel (d) marks the inset horizontal axis (from point A to E). The hybrid coordinate of the vertical cross section is terrain-following and can be linked to height above surface as follows: 1.0 is the surface, 0.95 is  $\sim 500\text{-m}$  agl, 0.90 is  $\sim 1\text{-km}$  agl, and 0.70 is  $\sim 3\text{-km}$  agl. The wind arrows in the vertical cross section do not show all the levels near surface for clarity. The arrows shown in the four panels and vertical cross-section represent wind in horizontal plane. Note that panel (d) shows a close-up over the west end of Lake Ontario.

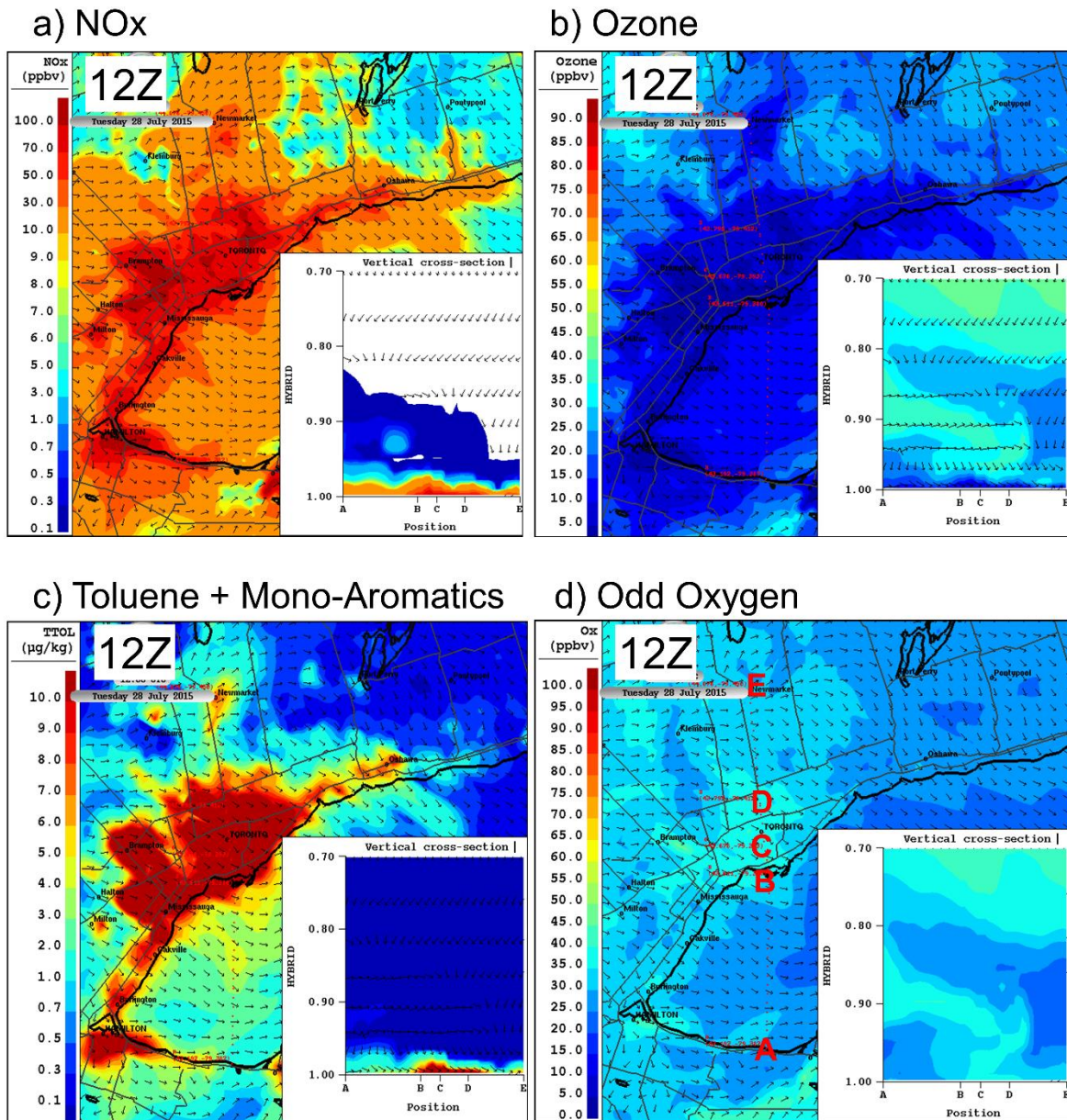


**Figure S11.** GEM-MACH-TEB predictions for air quality variables at 12:00 UTC 28 July 2015. Panels are for (a)  $\text{NO}_x$  (sum of  $\text{NO} + \text{NO}_2$ ), (b)  $\text{O}_3$ , (c) toluene (+other mono-substituted aromatics), and (d)  $\text{O}_x$  (sum of  $\text{O}_3 + \text{NO}_2$ ). The white line in panel (a) is the horizontal axis (from point A to E). Surface concentrations are shown in the main part of each panel while insets show vertical cross-sections of the same species (and for the same concentration contour intervals). Refer to Figure S10 for description of hybrid vertical coordinate.

At 15:00 UTC (11:00 a.m. local time), the land temperature rises and becomes higher than the lake temperature. Surface winds over the lake start to move on-shore, creating a weak lake-breeze front just inland along the Lake Ontario shoreline. The line of convection associated with the lake-breeze is evident in the vertical velocity field in Figure S12c (i.e., red-coloured cells along lakeshore). The mixing length in the vertical cross section is also enhanced at point 'C' over downtown Toronto. Low mixing heights are noted over the lake surface. The divergence in surface winds at the center of Lake Ontario results in weak subsidence. The winds in the residual layer remain from the northwest over the region and the winds at 3-km altitude remain from NNE. The winds over land are light and sporadic in direction.

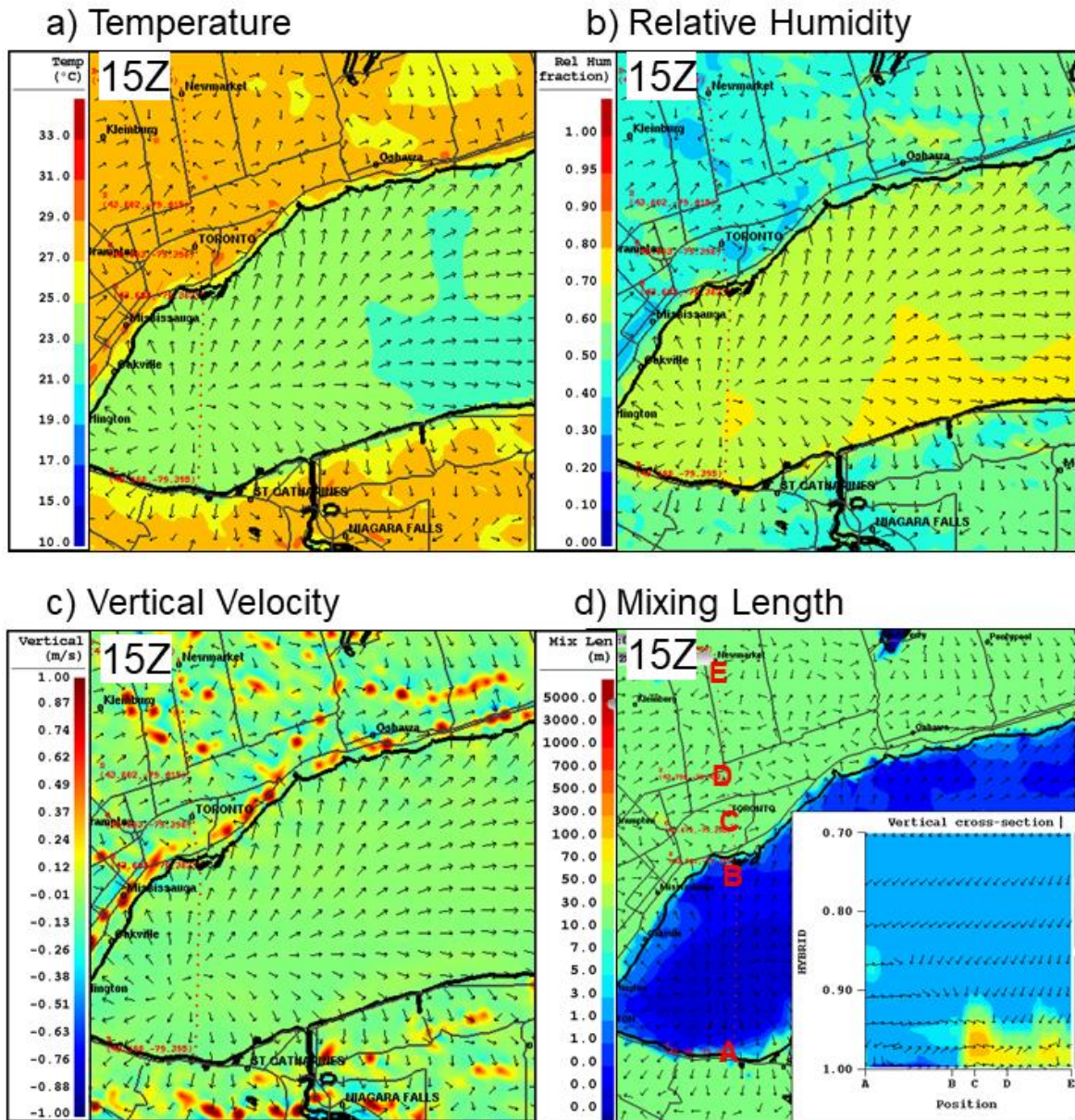


**Figure S12.** GEM-MACH-TEB predictions for meteorological variables at 15:00 UTC 28 July 2015. Refer to Figure S10 for description of hybrid vertical coordinate.

The pollutants over Lake Ontario begin to move back on-shore at 15:00 UTC (Figure S13). The lake-breeze convergence along the shoreline vertically transports the pollutants over downtown Toronto. A distinct high  $\text{NO}_x$  region is modelled between 1–2 km above the lakeshore over Toronto Island with the return flow at this altitude moving the air mass back over the lake. The modeled  $\text{NO}_x$  mixing ratio peaks at 9–10 ppbv with sharp gradients in concentration near the edges of the plume. The VOCs are also quite high in concentration (e.g., 4–5 ppbv for the mono-substituted aromatic lumped species, termed TOLU in GEM-MACH-TEB) in this elevated parcel. Local  $\text{O}_3$  production is evident in this plume (40–45 ppbv) compared to the surrounding air (25–30 ppbv).

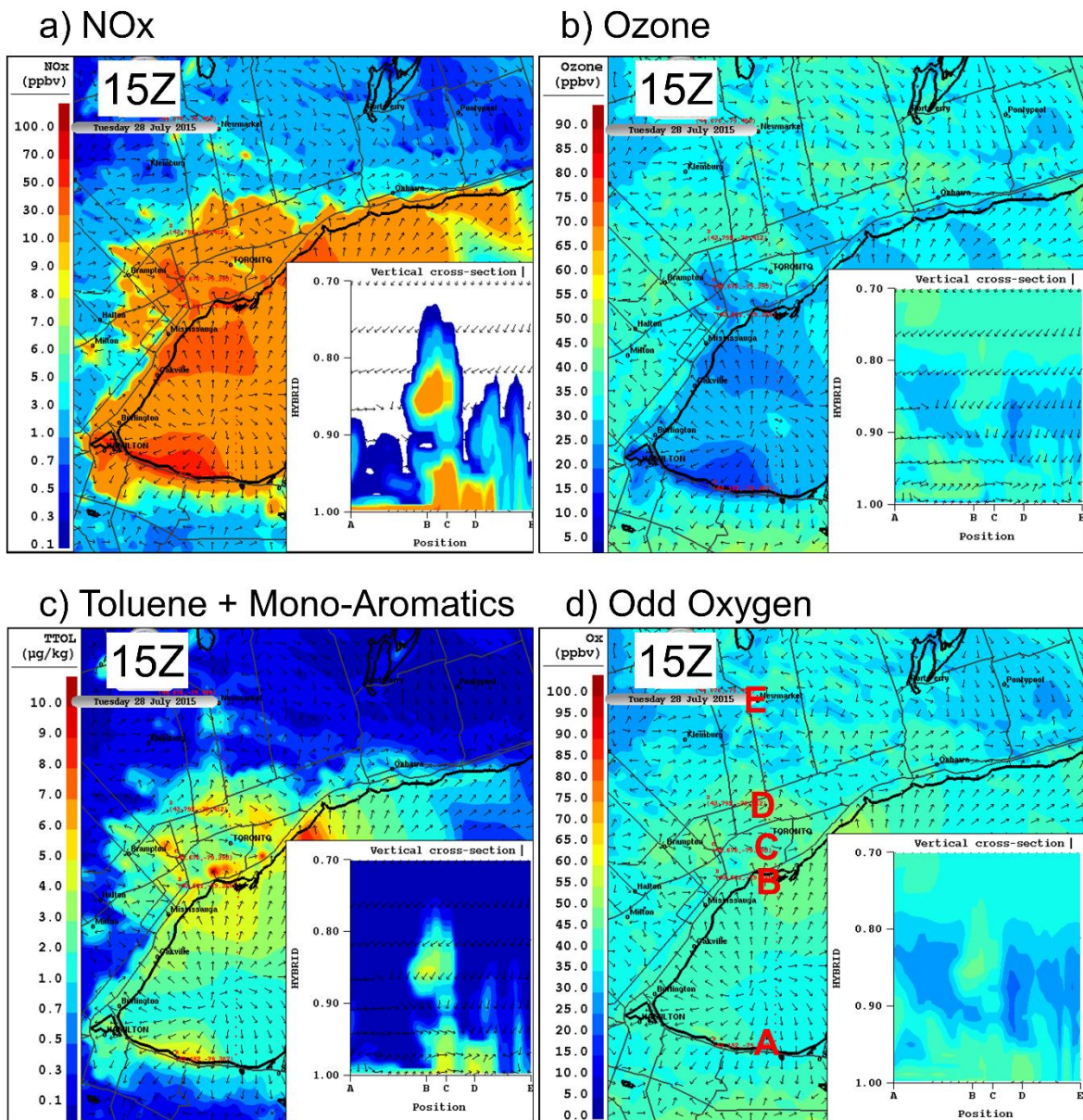


**Figure S13.** GEM-MACH-TEB predictions for air quality variables at 15:00 UTC 28 July 2015. Refer to Figure S10 for description of hybrid vertical coordinate.

At 18:00 UTC (02:00 p.m. local time), the temperature over land reaches 31 °C and a very strong modeled lake-breeze circulation has formed. The lake-breeze front reaches north of the Toronto city limit and all the way to Kleinburg, as noted by the modeled vertical wind at 300-m altitude in Figure S14c. In fact, the lake-breeze front goes all around the GTHA from Oshawa to Niagara. The cross section of mixing length shows elevated values over Downtown Toronto and the most intense convection just south of point 'E' in Richmond Hill. The elevated mixing length reaches up to 2.2-km above ground. Horizontal winds in the convection over Toronto are from the south, but switch from the north at 3-km altitude. Over Toronto Island, the lake-breeze circulation is shallow with return flow back over the lake remaining below 1-km height.

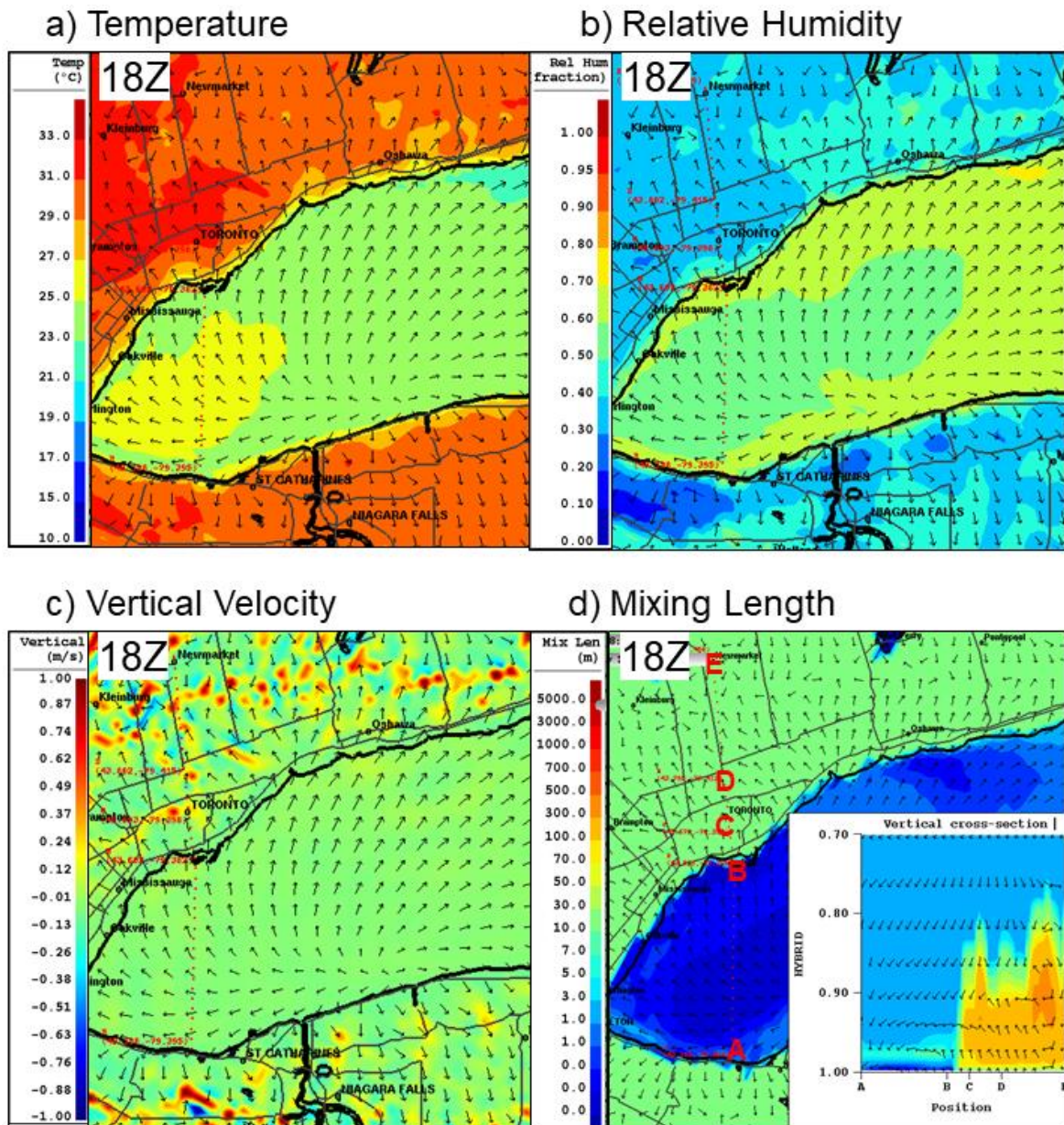


**Figure S14.** GEM-MACH-TEB predictions for meteorological variables at 18:00 UTC 28 July 2015. Refer to Figure S10 for description of hybrid vertical coordinate.

Strong  $O_3$  production is modeled in this shallow return flow over Toronto Island with maximum  $O_3$  up to 90 ppbv at 500-m altitude (Figure S15, 02:00 p.m. local time). The precursor  $NO_x$  and VOCs are also elevated in this shallow circulation. The  $O_3$  mixing ratio in the region of convergence along the lake-breeze front in North Toronto is predicted to reach 65–75 ppbv in the convection all the way up to 2.5-km altitude.

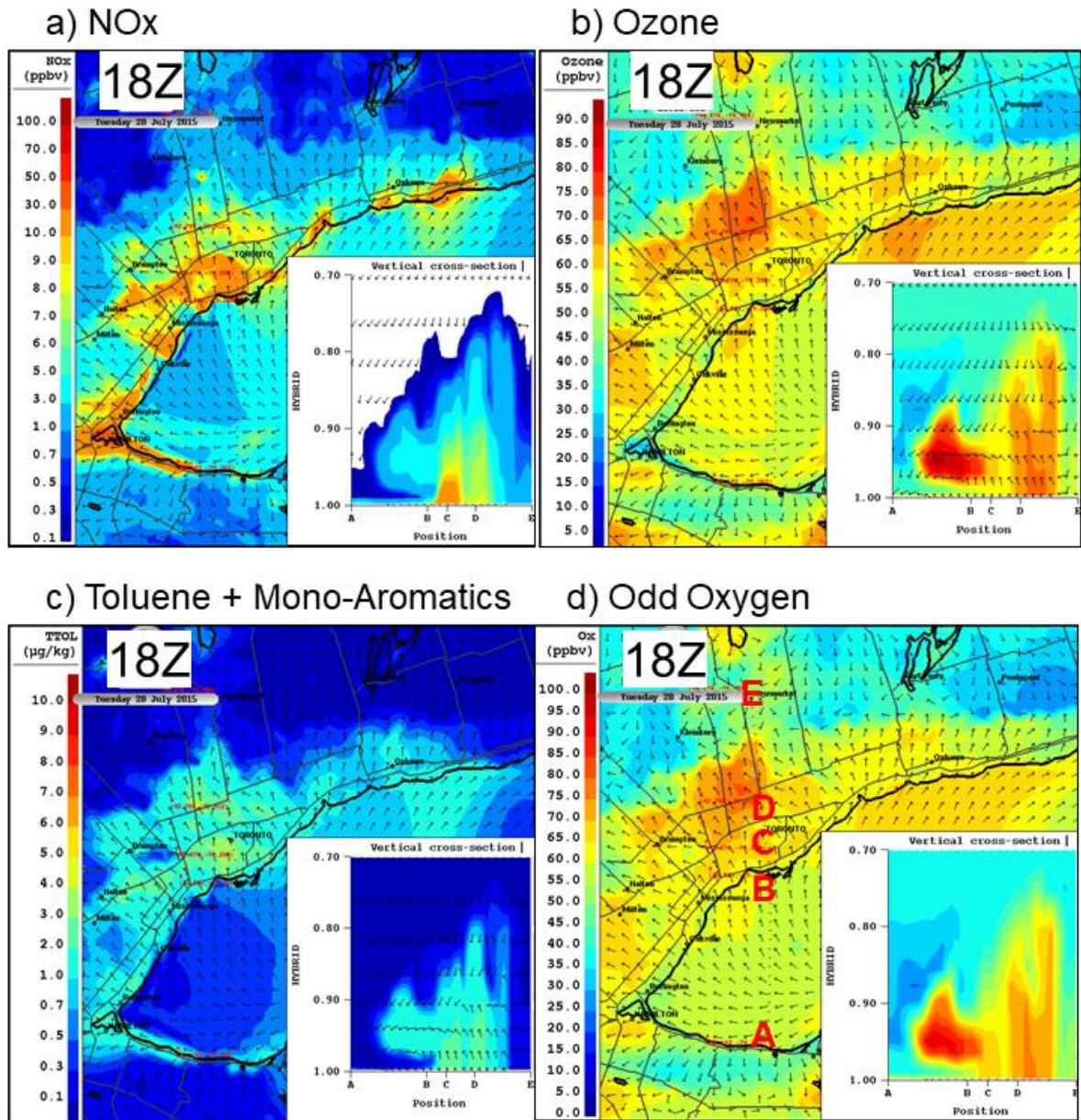


**Figure S15.** GEM-MACH-TEB predictions for air quality variables at 18:00 UTC 28 July 2015. Refer to Figure S10 for description of hybrid vertical coordinate.

## 2.5-km GEM-MACH-TEB Modeled Wind Fields on 12 July 2015

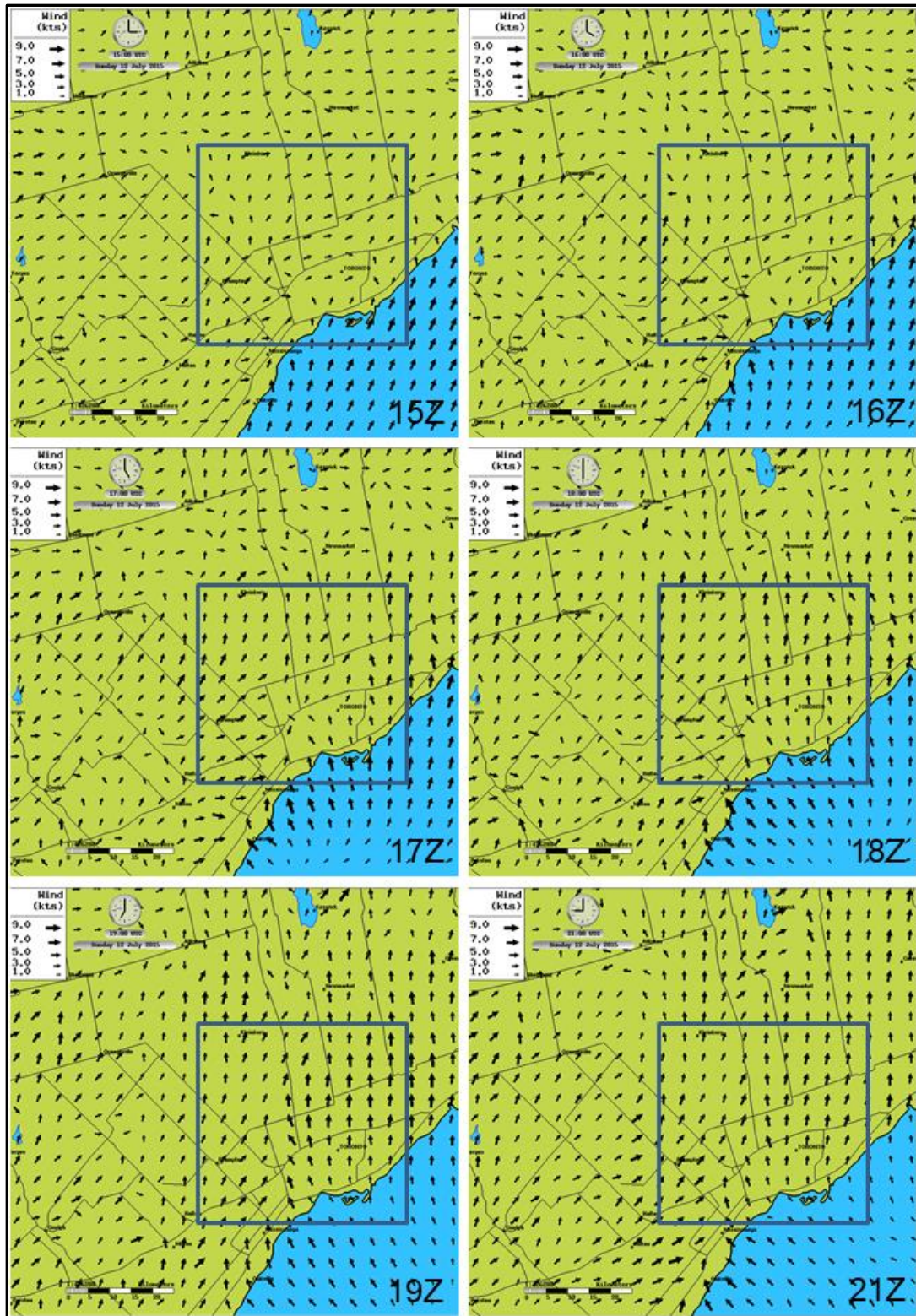


**Figure S16.** Modeled winds fields for the afternoon of 12 July 2015. The box is the same area of interest as in Figures 18 and 19 in main text. The black line denotes the lakeshore and the grey lines mark major roads.

Comparison of 2.5-km GEM-MACH-TEB Sea-Level Pressure with the 10-km GEM Regional Analysis

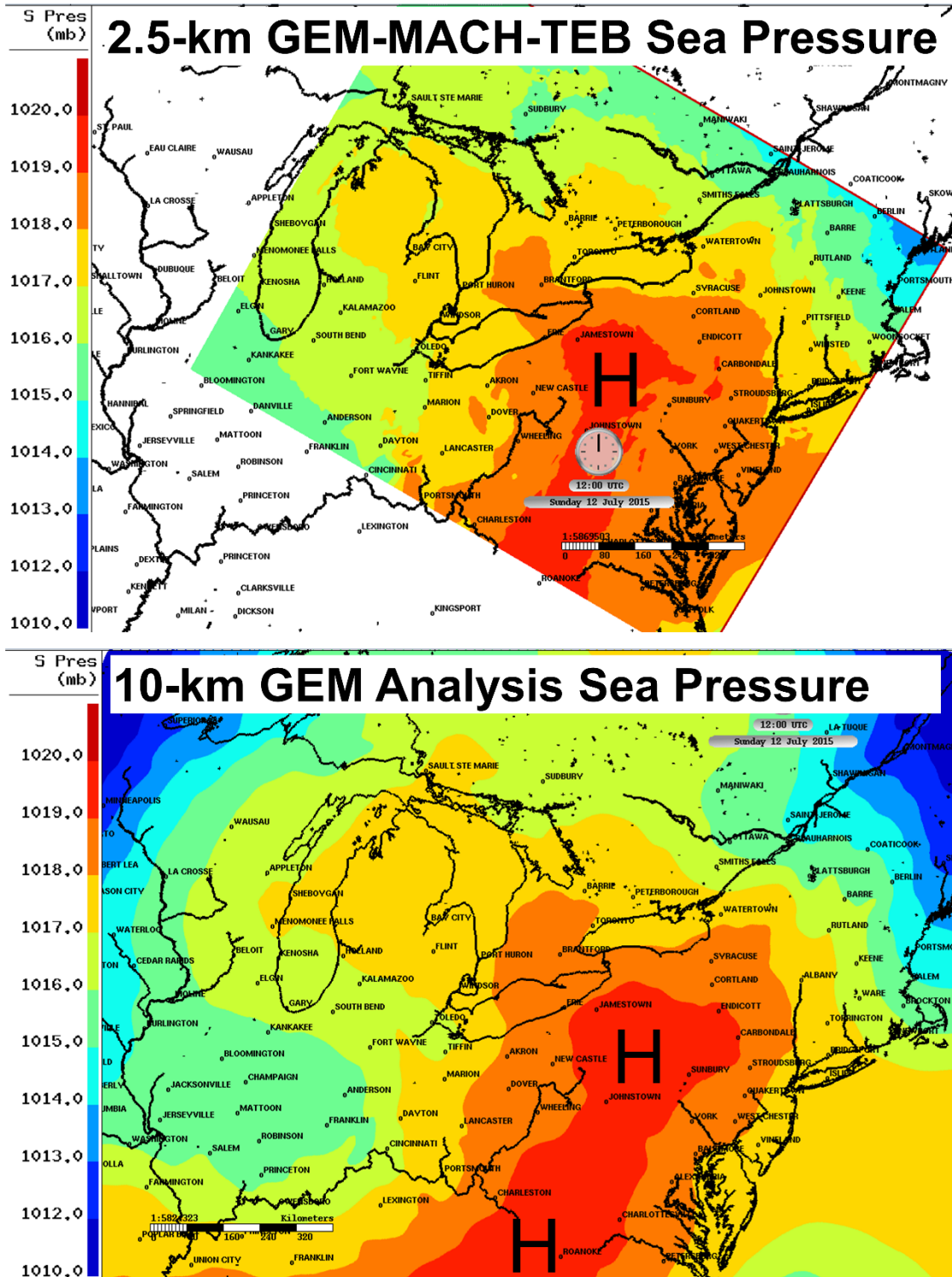


Figure S17. Comparison of 2.5-km GEM-MACH-TEB Sea-Level Pressure map with the 10-km GEM Analysis map for 12 July 2015 at 12 GMT. The regional-scale meteorology leading into the case study is predicted reasonably. The 10-km pressure analysis compares reasonably to the coarser resolution, synoptic-scale NCEP analysis in Figure 9 in main text.

## References

1. APEI, 2015. Air Pollutant Emission Inventory (APEI) Report 1990–2015. Environment and Climate Change Canada February, 2015. Available online: <http://www.publications.gc.ca/site/eng/9.810709/publication.html> (accessed on 27 May 2019).
2. AMPD, Air Market Program Data, Acid Rain Program. United States Environmental Protection Agency. April 2017. Available online: <https://ampd.epa.gov/ampd/> (accessed on 26 August 2019).
3. MOECC, 2015. Air Quality in Ontario Report. Ontario Ministry of the Environment and Climate Change. Available online: <http://www.airqualityontario.com/press/publications.php> (accessed on 26 August 2019).
4. APETD, Air Pollutant Emissions Trends Data. United States Environmental Protection Agency April, 2017. Available online: [www.epa.gov/air-emissions-inventories/air-pollutant-emissions-trends-data](http://www.epa.gov/air-emissions-inventories/air-pollutant-emissions-trends-data) (accessed on 15 September 2019).
5. Yu, S.; Mathur, R.; Schere, K.; Kang, D.; Pleim, J.; Otte, T.L. A detailed evaluation of the Eta-CMAQ forecast model performance for O<sub>3</sub>, its related precursors, and meteorological parameters during the 2004 ICARTT study. *J. Geophys. Res. Atmos.* **2007**, *112*, D12S14.
6. Dennis, R.; Fox, T.; Fuentes, M.; Gilliland, A.; Hanna, S.; Hogrefe, C.; Irwin, J.; Rao, S.T.; Scheffe, R.; Schere, K.; et al. A framework for evaluating regional-scale numerical photochemical modeling systems. *Environ. Fluid Mech.* **2010**, *10*, 471–489.
7. Rao, S.T.; Galmarini, S.; Puckett, K. Air quality model evaluation international initiative (AQMEII): Advancing the state of the science in regional photochemical modeling and its application. *Bull. Am. Meteorol. Soc.* **2011**, *92*, 23–30.
8. Simon, H.; Baker, K.R.; Phillips, S. Compilation and interpretation of photochemical model performance statistics published between 2006 and 2012. *Atmos. Environ.* **2012**, *61*, 124–139.
9. Russell, M.; Hakami, A.; Makar, P.A.; Akingunola, A.; Zhang, J.; Moran, M.D.; Zheng, Q. An evaluation of the efficacy of very high resolution air-quality modelling over the Athabasca oil sands region, Alberta, Canada. *Atmos. Chem. Phys.* **2019**, *19*, 4393–4417.
10. Foley, T.; Betterton, E.A.; Robert Jacko, P.E.; Hillery, J. Lake Michigan air quality: The 1994–2003 LADCO Aircraft Project (LAP). *Atmos. Environ.* **2011**, *45*, 3192–3202.
11. Cleary, P.A.; Fuhrman, N.; Schulz, L.; Schafer, J.; Fillingham, J.; Bootsma, H.; McQueen, J.; Tang, Y.; Langel, T.; McKeen, S.; et al. Ozone distributions over southern Lake Michigan: Comparisons between ferry-based observations, shoreline-based DOAS observations and model forecasts. *Atmos. Chem. Phys.* **2015**, *15*, 5109–5122.
12. Qin, M.; Yu, H.; Hu, Y.; Russell, A.G.; Odman, M.T.; Doty, K.; Pour-Biazar, A.; McNider, R.T.; Kniing, E. Improving ozone simulations in the Great Lakes Region: The role of emissions, chemistry, and dry deposition. *Atmos. Environ.* **2019**, *202*, 167–179.
13. Dunlea, E.J.; Herndon, S.C.; Nelson, D.D.; Volkamer, R.M.; San Martini, F.; Sheehy, P.M.; Zahniser, M.S.; Shorter, J.H.; Wormhoudt, J.C.; Lamb, B.K.; et al. Evaluation of nitrogen dioxide chemiluminescence monitors in a polluted urban environment. *Atmos. Chem. Phys.* **2007**, *7*, 2691–2704.
14. U.S. EPA. *Guidance on the Use of Models and Other Analyses for Demonstrating Attainment of Air Quality Goals for Ozone PM<sub>2.5</sub> and Regional Haze*; United States Environmental Protection Agency: Washington, DC, USA, 2007; p. 253.
15. Chang, L.T.-C.; Duc, H.N.; Scorgie, Y.; Trieu, T.; Monk, K.; Jiang, N. Performance evaluation of CCAM-CTM regional airshed modelling for the New SouthWales Greater Metropolitan Region. *Atmosphere* **2018**, *9*, 486.
16. Geddes, J.A.; Murphy, J.G.; Wang, D.K. Long term changes in nitrogen oxides and volatile organic compounds in Toronto and the challenges facing local ozone control. *Atmos. Environ.* **2009**, *43*, 3407–3415.
17. Brook, J.R.; Makar, P.A.; Sills, D.M.L.; Hayden, K.L.; McLaren, R. Exploring the nature of air quality over southwestern Ontario: Main findings from the Border Air Quality and Meteorology Study. *Atmos. Chem. Phys.* **2013**, *13*, 10461–10482.